

# Experimental studies on self-propagating combustion synthesis of niobium nitride

C.L. Yeh\*, H.C. Chuang

*Department of Mechanical and Automation Engineering, Da-Yeh University, 112 Shan-Jiau Road, Da-Tsuen, Changhua 51505, Taiwan, ROC*

Received 1 September 2003; received in revised form 9 September 2003; accepted 2 October 2003

Available online 17 March 2004

## Abstract

An experimental investigation of self-propagating high-temperature synthesis (SHS) of niobium nitride (NbN) was conducted with niobium compacts in gaseous nitrogen. A detailed characterization of the flame propagation mode was performed in this study. Effects of sample density, nitrogen pressure, and diluent content on the degree of conversion, flame-front velocity, and combustion temperature were studied. It was found that the self-sustained combustion of the niobium/nitrogen SHS process was featured by the spinning combustion wave traveling on the sample surface. Prior to the self-sustained combustion stage, the igniter heat input contributed the longitudinal propagation of a planar front. The flame-front velocity increased with nitrogen pressure, but decreased with sample density. Measured temperature profiles and SEM examinations showed that the sample remained in solid phase, implying that the sample retained its porosity for the filtration of nitrogen gas in the afterburning stage. For the undiluted samples, the conversion percentages ranged between 56 and 70% were independent of the nitrogen pressure, due to the afterburning nitridation. The addition of diluent optimally yielded an increase of about 13% in the degree of conversion. The XRD analysis indicated that the dominant nitride phase synthesized in this study was  $\delta$ -NbN. For the undiluted samples, a small amount of  $\beta$ -Nb<sub>2</sub>N was found in the combustion product.

© 2003 Elsevier Ltd and Techna Group S.r.l. All rights reserved.

**Keywords:** Niobium nitride; SHS; Spin combustion; Afterburning; Diluent

## 1. Introduction

Nitrides of transition metals of groups IV(B) and V(B) have been considerably investigated because of their unique chemical and physical properties, such as high melting point, chemical inertness, superior hardness, and metallic electrical conductivity [1]. Among these nitrides, niobium nitride (NbN) is featured by a relatively high superconducting transition temperature [2]. From the viewpoint of the electron emission property, NbN has been proven to be an excellent candidate of the field emitter applied to electron beam systems [3,4]. Because of the high heat of reaction between transition metal and nitrogen, nitrides of some transition metals can be obtained by means of the combustion synthesis, in which chemical reactions and structure formation take place [5]. Combustion synthesis has been recognized as an attractive alternative of producing advanced materials to the con-

ventional methods, which, in general, are time-consuming and energy intensive [6]. More than 500 kinds of materials, including carbides, borides, silicides, nitrides, sulfides, hydrides, intermetallics, and many complex composites have been synthesized by applying the combustion synthesis process not only for solid–solid systems, but also for solid–gas and/or solid–liquid systems [5–7]. Since there is usually far less of the gaseous reagent in the pores of the sample than is needed for combustion, the gaseous reagent has to be delivered to the combustion zone by filtration through the porous structure of the solid reactant. Filtration is believed to occur spontaneously on account of the pressure difference caused by the absorption of gaseous reagent in the combustion front [2].

The production of transition metal nitrides by combustion synthesis can either be accompanied by melting of the metal reactant or nitride product, or it can be completed without the formation of any liquid phase [8]. For example, titanium (Ti) exhibits excessive melting upon combustion in nitrogen, whereas tantalum (Ta) remains in the solid phase [8]. Melting of reactant powders reduces the permeability of samples

\* Corresponding author. Tel.: +886-4-8511888x2118;  
fax: +886-4-8511215.

E-mail address: clyeh@mail.dyu.edu.tw (C.L. Yeh).

and thereby hinders the filtration of nitrogen. Therefore, dilution of the metal reactant with the final nitride product is suggested as an effective means to lower the sample temperature, to suppress the melting, and then to increase the degree of conversion [9]. Moreover, the addition of product nitride powders in the reactant mixture will not cause any variation in the homogeneity of the combustion product. For the situation without the formation of any liquid phase, the overall conversion percentage can also be increased by adding the product nitride as a diluent, since the diluent is inert and consumes no nitrogen.

The synthesis of refractory inorganic compounds, including titanium, zirconium, niobium, and hafnium nitrides,

by the SHS process was pioneered by Merzhanov and Borovinskaya [2]. The original experiments were carried out in gaseous nitrogen with porous samples pressed from metal powders. Among the early transition metals, the titanium/nitrogen system has been extensively investigated by SHS [8–12]. However, much less SHS study associated with the niobium/nitrogen system has been reported. Zhang and Munir [13] investigated the effects of sample porosity and nitrogen pressure on the SHS of niobium nitride with the use of compacted niobium powders in the form of cylindrical pellets. It was found that at low pressures (<2.7 atm) the dominant nitride phase was  $\text{Nb}_3\text{N}_4$ , but at higher pressures (3.4–13.6 atm) the major nitride phase in the surface

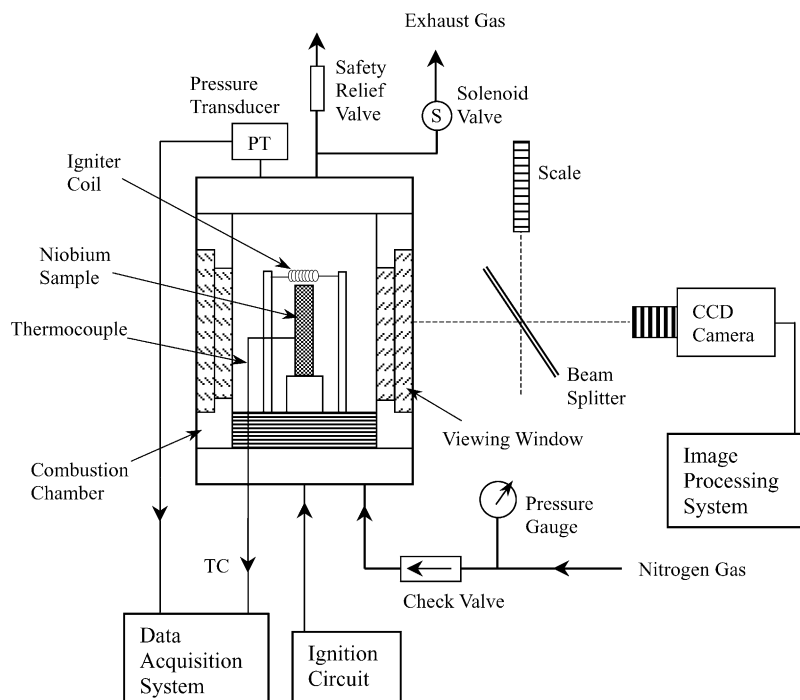


Fig. 1. Schematic diagram of experimental setup to study SHS of niobium nitride.

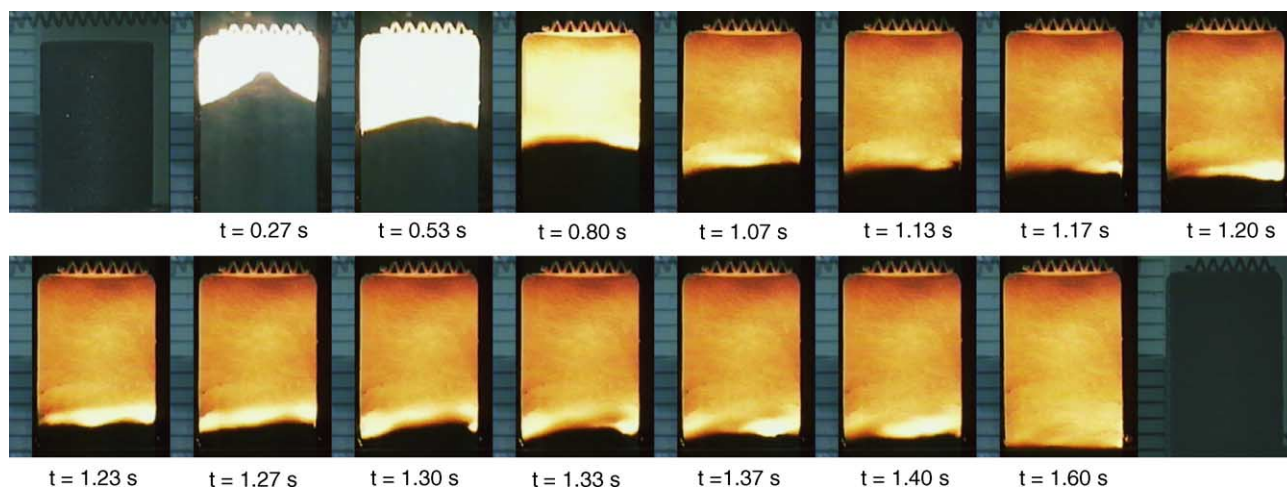


Fig. 2. Recorded burning images indicating spinning combustion wave on an undiluted 50% TMD Nb sample in 0.62 MPa  $\text{N}_2$ .

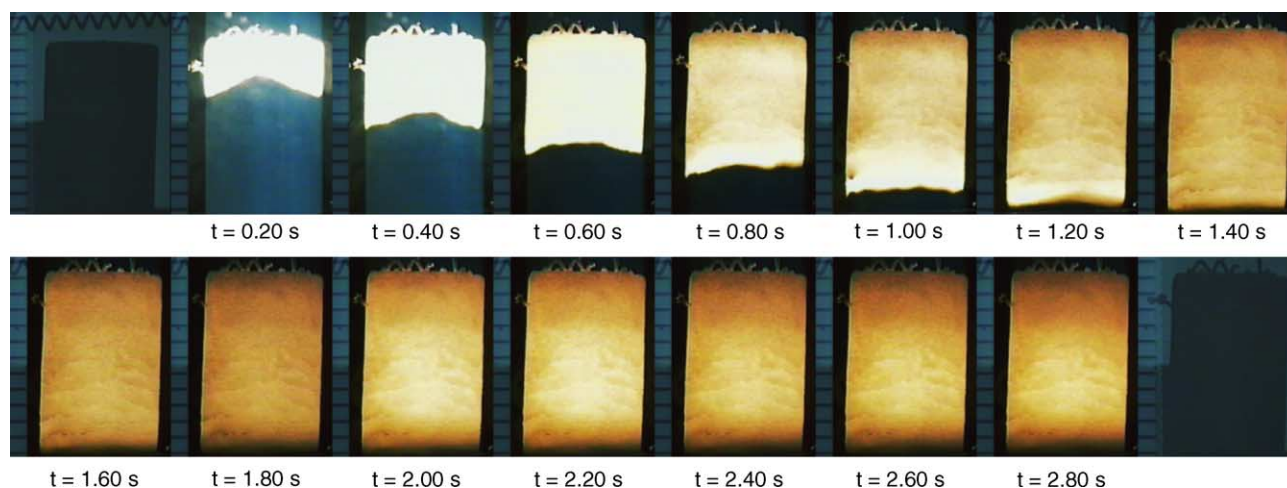


Fig. 3. Recorded burning images indicating afterburning phenomenon on an undiluted 50% TMD Nb sample in 0.96 MPa  $N_2$ .

layer was NbN. In order to lower the filtration resistance of compacted samples, Agrafiotis et al. [14] conducted the synthesis of niobium nitride in nitrogen of 5–100 atm using loosely packed niobium powders in the form of porous beds. With this configuration, almost complete conversion of Nb to NbN was achieved under the solid-phase dilution with 10–20 wt.% NbN in the reactant mixture.

The objective of this research was to experimentally investigate the combustion synthesis of niobium nitride in the SHS mode with compacted niobium samples in gaseous nitrogen. Combustion characteristics, such as the propagation mode of self-sustained combustion front, flame-front velocity, combustion temperature profile, and afterburning reaction, were studied to establish a fundamental knowledge of the SHS process for the production of niobium nitride. Effects of the sample density, nitrogen pressure, and solid-phase dilution on the conversion percentage, combustion temperature, and flame-front propagation velocity were also explored. In addition, the composition analysis and morphology examination of final products obtained under different nitrogen pressures and diluent contents were performed.

## 2. Experimental

### 2.1. Test samples

Niobium (Nb) powders (Strem Chemicals, –325 mesh) of 99.8% purity were used as the reactant in this study and were pressed into cylindrical specimens having a diameter of 7 mm and a height of 12.5 mm. In order to obtain test samples with different porosities, the niobium compacts were formed with the green packing densities equal to 50, 55, and 60% of the theoretical maximum density (TMD) of niobium ( $8.6 \text{ g/cm}^3$ ).

For the preparation of samples that contained the final product NbN as a diluent, both Nb and NbN powders were dry mixed in a ball mill for 10 h. The diluent content was

ranged from 5 to 25% by weight of the total powder mixture. The NbN-diluted sample compacts were prepared to have the density equal to 55% TMD of the powder mixture. After the combustion, the conversion percentage of metal to nitride was calculated from the measurement of weight change of sample compacts assuming a stoichiometric nitride as the final product [8–14].

### 2.2. Experimental setup and instrumentation

The reaction between the niobium sample and nitrogen gas was carried out in a stainless-steel windowed combustion chamber (Fig. 1) under a nitrogen pressure ranging from 0.27 to 1.5 MPa. The nitrogen gas used in this study had a purity of 99.999%. The ignition of niobium samples was accomplished by a heated tungsten coil with a voltage of 65 V and a current of 1.5 A. Two windows on the combustion chamber provided visual monitoring, as well as optical

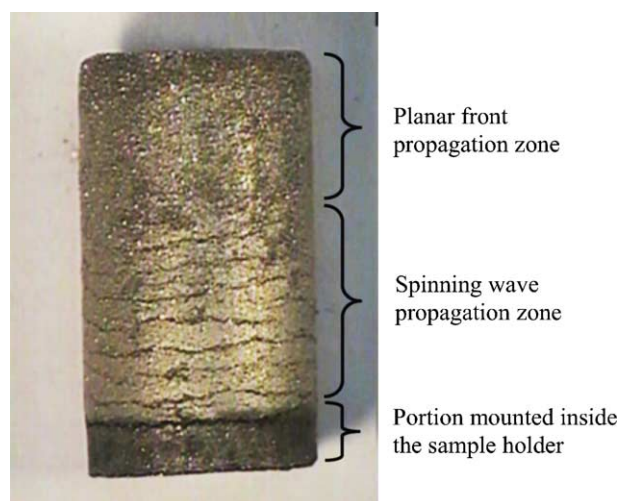


Fig. 4. Photograph of a combustion product obtained from an undiluted 50% TMD Nb sample nitrided in 0.79 MPa  $N_2$ .

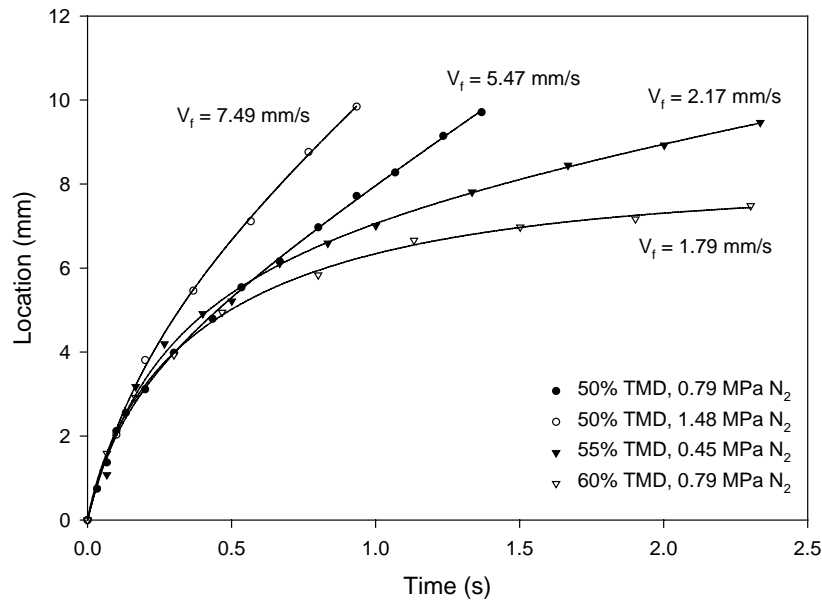


Fig. 5. Flame-front trajectories of undiluted Nb samples under different test conditions.

diagnostics. Before the experiment, the chamber was evacuated down to 0.1 Torr and then flushed with the nitrogen gas for 2–3 min. After that, the chamber was filled with nitrogen up to the desired pressure.

The propagation rate of combustion front was measured by the recording of the whole combustion event with a color CCD video camera (Pulnix TMC-7) at 30 frames/s. Due to the extremely high intensity of light emission during the reaction between niobium and nitrogen, the exposure time of each recorded image was set at 0.1 ms. To facilitate the accurate measurement of instantaneous locations of the com-

bustion front, a beam splitter (Rolyn Optics), with a mirror characteristic of 75% transmission and 25% reflection, was used to optically superimpose a scale onto the image of the niobium compact. The temperature of niobium sample was measured by a fine-wire (125  $\mu\text{m}$ ) Pt/Pt–13%Rh thermocouple (Omega Inc.) attached on the sample surface. The variation of chamber pressure during the test was monitored by a pressure transducer.

The burned samples were recovered and weighed. The microstructure of combustion product was examined under a scanning electron microscope (SEM). The chemical

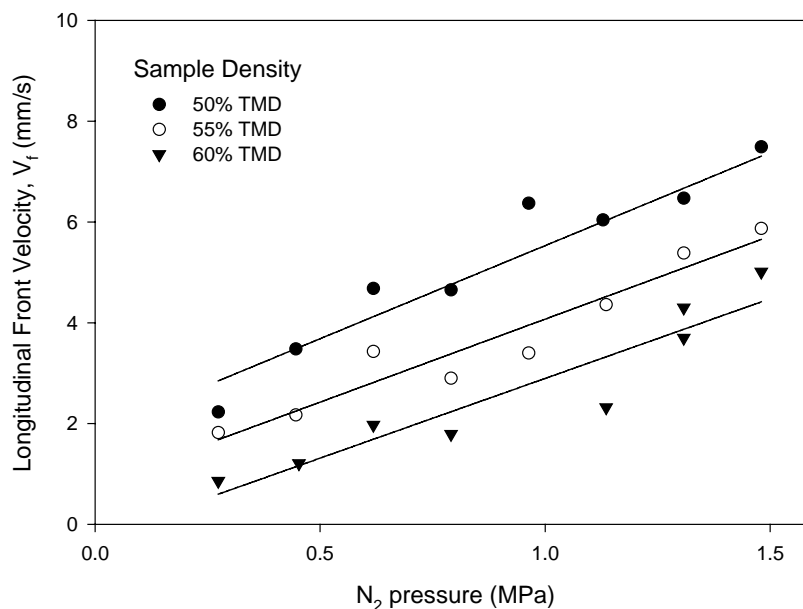


Fig. 6. Effects of nitrogen pressure and sample density on longitudinal flame-front velocity of undiluted Nb samples.

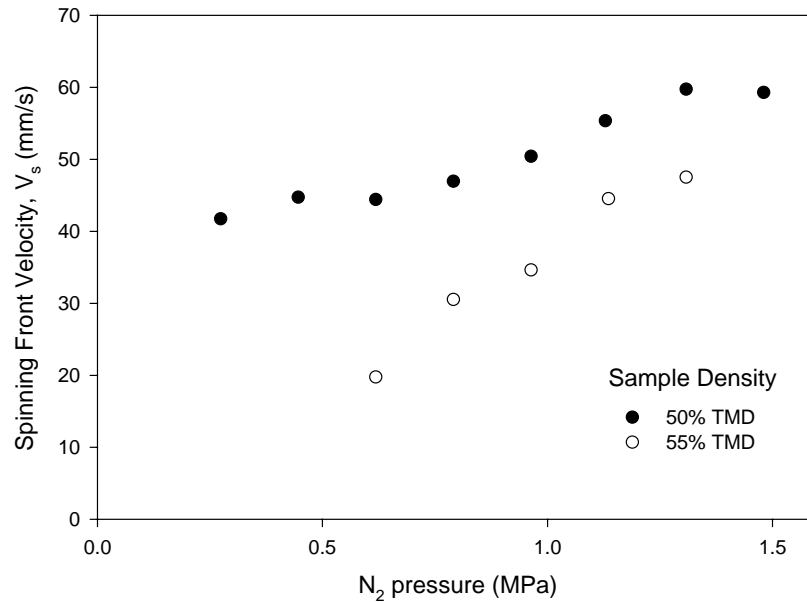


Fig. 7. Effects of nitrogen pressure and sample density on spinning front velocity of undiluted Nb samples.

composition of burned samples was identified by an X-ray diffractometer (Mac Science MXP) with Cu K $\alpha$  radiation operating at 40 kV.

### 3. Results and discussion

#### 3.1. Observation of combustion characteristics

Fig. 2 shows a set of typical recorded images illustrating the propagation of the combustion wave of an undiluted niobium sample nitrided in gaseous nitrogen of 0.62 MPa. It

is evident in Fig. 2 that upon ignition a distinct flame-front propagates downward from the ignited top plane, and transforms the cold reactant to an incandescent combustion product. The luminosity on the burned portion of the test sample is very strong at the early stage. Subsequently, at time ( $t$ ) about 0.8 s, the brightness of the burned portion decreases and the flame-front forms a localized combustion zone moving along a spiral trajectory on the sample surface. The reaction zone travels not only transversely but also longitudinally at this stage. As shown in Fig. 2, the spinning combustion wave is clearly observable between  $t = 1.07$  and 1.40 s. It was believed that before the appearance of

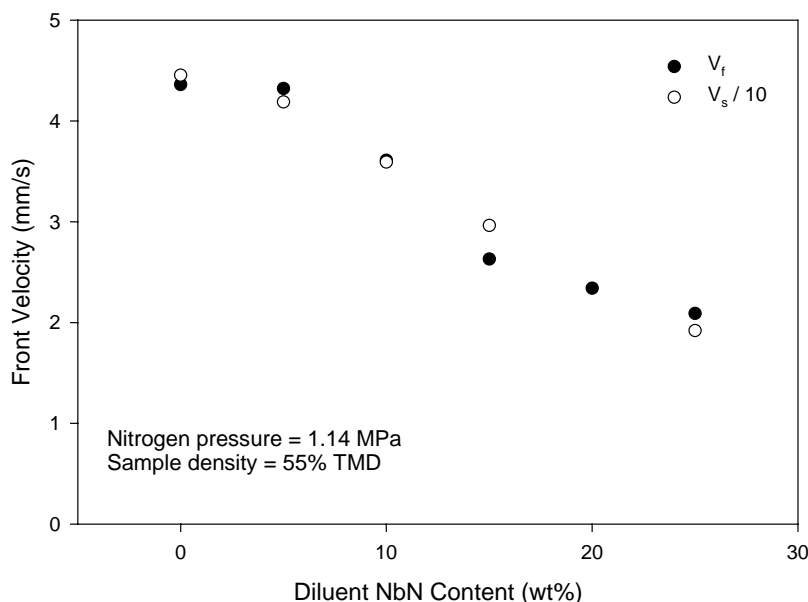


Fig. 8. Effect of diluent concentration on longitudinal and spinning front velocities of Nb samples.

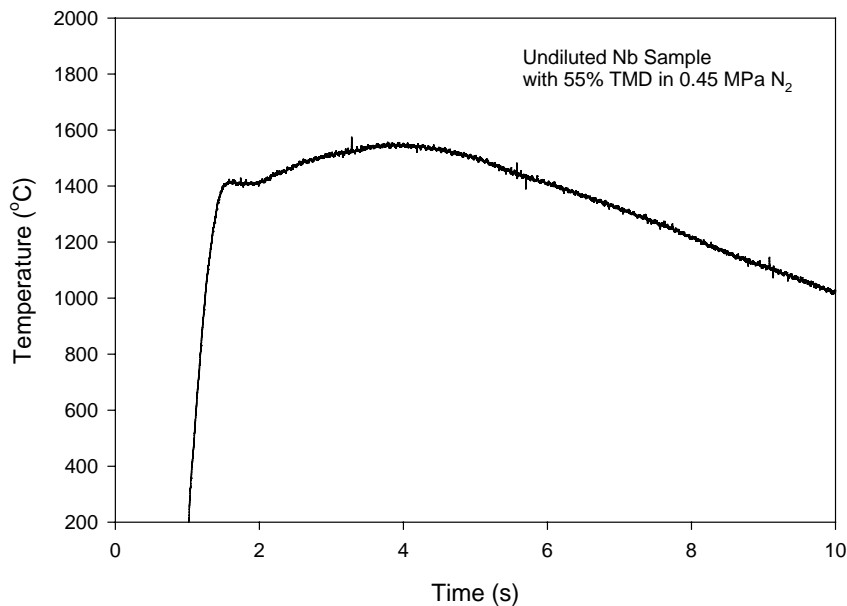


Fig. 9. Measured temperature profile of an undiluted 55% TMD Nb sample nitrided in 0.45 MPa  $N_2$ .

spinning waves the thermal energy liberated from both the tungsten coil igniter and the Nb/ $N_2$  reaction assisted the propagation of the flame-front. The combustion then became self-sustained with the fading of the igniter heat input. According to Ivleva and Merzhanov [15], when the heat flux from the self-sustained combustion is insufficient to maintain the steady propagation of a planar front, the flame-front forms one or several localized reaction zones. Therefore, it is proposed from the above observations that the reaction front associated with the SHS of niobium nitride in the self-sustained regime propagates in a spinning mode.

Besides the spinning combustion wave, the SHS process of the niobium/nitrogen system is characterized by the afterburning phenomenon, which means that the reaction takes place after the passage of the flame-front. As shown in Fig. 3, the flame-front reaches the bottom of the sample at  $t = 1.4$  s, beyond which the brightness gradually vanishes from the sample. The luminosity on the burned sample becomes very dim at  $t = 1.8$  s. However, at  $t = 2.0$  s the test sample appears to reglow, implying that the reaction resumes. The afterburning luminosity on the sample is clearly noticeable during the time period of 2.0–2.8 s. This observation

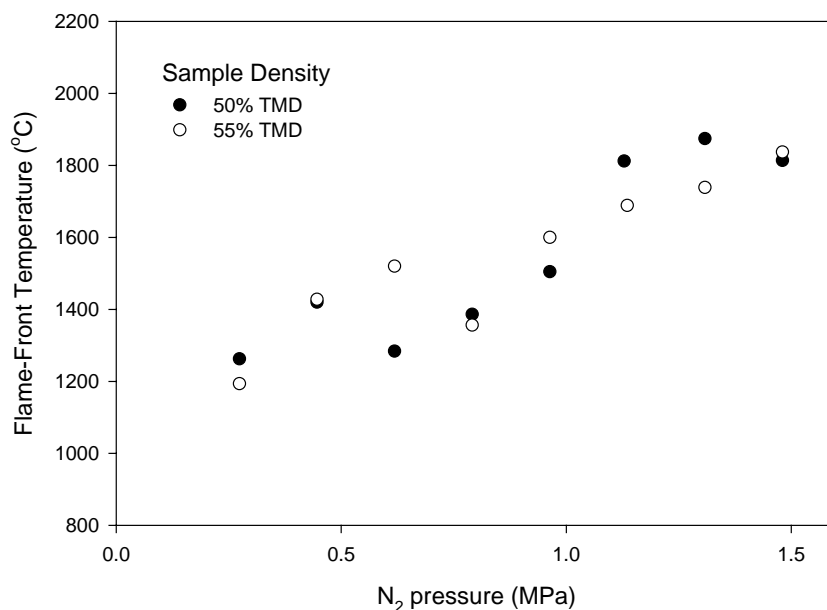


Fig. 10. Effects of nitrogen pressure and sample density on flame-front temperature of undiluted Nb samples.



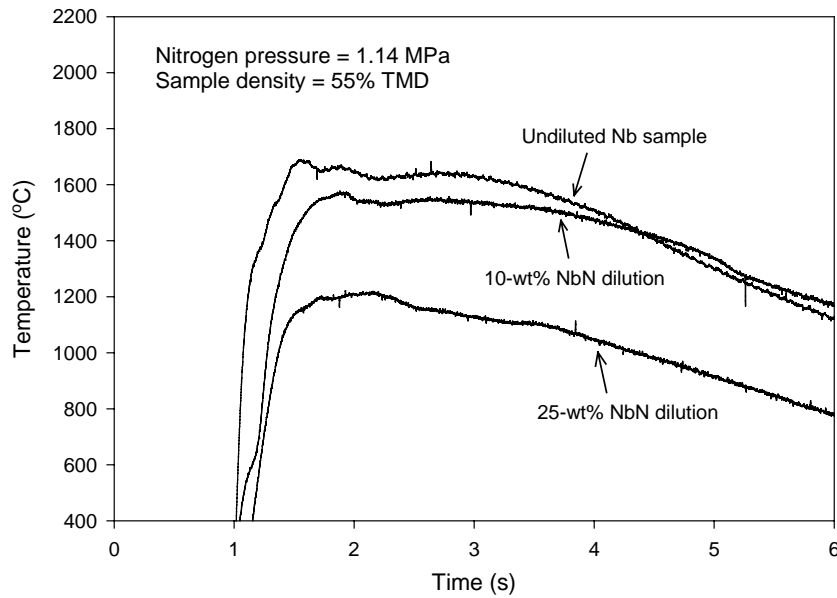


Fig. 11. Effect of diluent concentration on combustion temperature of Nb samples in 1.14 MPa  $N_2$ .

provides a visual evidence of the afterburning stage, where a prolonged bulk post-combustion occurs. It was believed that in this study the afterburning reaction should contribute appreciably to the conversion of niobium to nitride, since the nitridation at the spinning combustion front was mostly confined on the sample surface.

Due to the propagation of the spinning combustion wave, the surface of the burned sample was left with visible spiral marks, as shown in Fig. 4. Except for the bottom portion of the sample, the external appearance of the burned sample exhibits two consecutive combustion stages including a planar front propagation zone and a spinning wave propagation

zone. The bottom portion mounted inside the sample holder was considered almost unreacted, because of the heat loss and lack of nitrogen.

### 3.2. Measurement of flame-front trajectory and propagation velocity

Based upon the above observations, two types of propagation velocities were deduced from the recorded images in this study. One is the longitudinal propagation velocity ( $V_f$ ) of the combustion front, and the other is the spinning velocity ( $V_s$ ) of the localized reaction zone. Fig. 5 shows

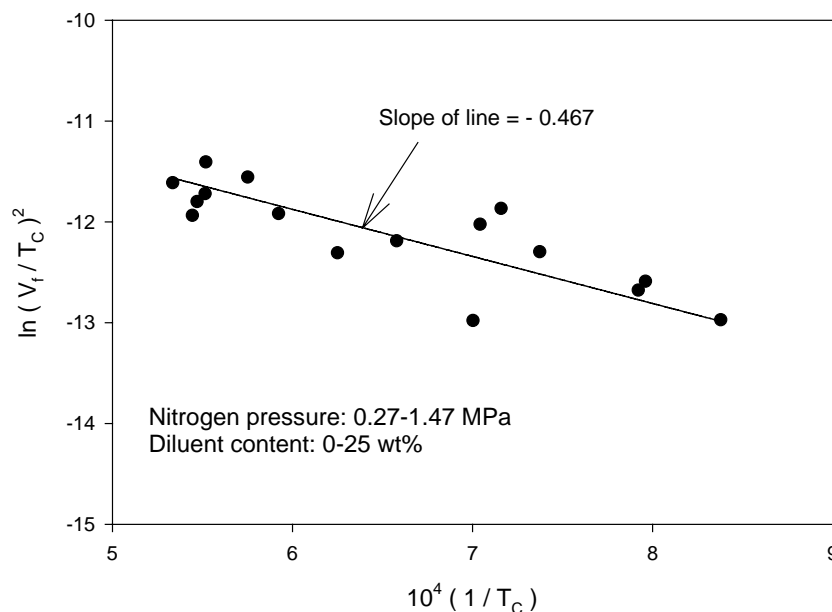


Fig. 12. Relation between flame-front velocity and combustion temperature for determination of activation energy of Nb/ $N_2$  SHS system.

a plot of longitudinal flame-front trajectories of undiluted Nb samples under different test conditions. The trajectory indicates that the flame-front velocity in the axial direction is relatively high right after the ignition and then experiences a noticeable deceleration, finally arriving at a nearly constant value. The high propagation velocity in the early stage was mainly attributed to the external heat flux from the igniter, and the later phase featuring a constant velocity represented the self-sustained combustion regime, where a spinning wave traveled both transversely and longitudinally. The values of  $V_f$  marked in Fig. 5 stand for the longitudinal front velocity in the self-sustained burning zone.

Fig. 6 presents the effects of nitrogen pressure and sample density on the longitudinal flame-front velocity ( $V_f$ ) of undiluted niobium samples in the self-sustained combustion regime. It is found that the flame-front velocity ( $V_f$ ) increases with nitrogen pressure, due to an increase of the initial nitrogen concentration within the porous sample. Moreover, the flame-front velocity increases with decreasing sample density, since a lower sample density means a better permeability for nitrogen gas to penetrate. The dependence of the spinning front velocity ( $V_s$ ) on sample density and nitrogen pressure for the undiluted samples is shown in Fig. 7. Similar to the longitudinal front velocity, the spinning velocity increases with nitrogen pressure, but decreases with sample density. Nevertheless, the spinning wave propagates at one order of magnitude faster than does the longitudinal one. It should be noted that the spinning velocity of 60% TMD Nb samples was not reported in Fig. 7, because the light intensity on the spinning hot zone of 60% TMD samples was too low to precisely deduce the velocity data.

Fig. 8 shows the decrease of both longitudinal and spinning front velocities with increasing diluent concentration. This was caused by the fact that the combustion temperature decreases with an increase in the diluent content. In agreement with the undiluted samples, the velocity of spinning wave is about 10 times larger than the longitudinal front velocity. However, for the samples diluted with 30-wt.% NbN or higher, it was found that the reaction was quenched before reaching the self-sustained combustion regime.

### 3.3. Measurement of combustion temperature

Fig. 9 shows a typical temperature profile measured in the self-sustained combustion stage of an undiluted Nb sample with 55% TMD in 0.45 MPa nitrogen. The rapid rise in temperature signifies the arrival of the localized reaction zone (i.e. the spinning wave) and the subsequent temperature increase followed by a gradual decline represents a prolonged post-combustion stage (i.e. the afterburning period). It is important to note that in this study measured sample temperatures during both flame-propagation and afterburning stages are lower than the melting points of Nb (2468 °C) and NbN (2300 °C). The temperature of the reaction front, in general, is increased by increasing the nitrogen pressure, as shown in Fig. 10. The variation of sample

densities (50 and 55% TMD) produces nearly no effect on the flame-front temperature. The effect of solid-phase dilution on the combustion temperature is shown in Fig. 11. As anticipated, the combustion temperature was decreased by increasing the diluent concentration. Fig. 11 also indicates a substantial decrease in combustion temperature for the sam-

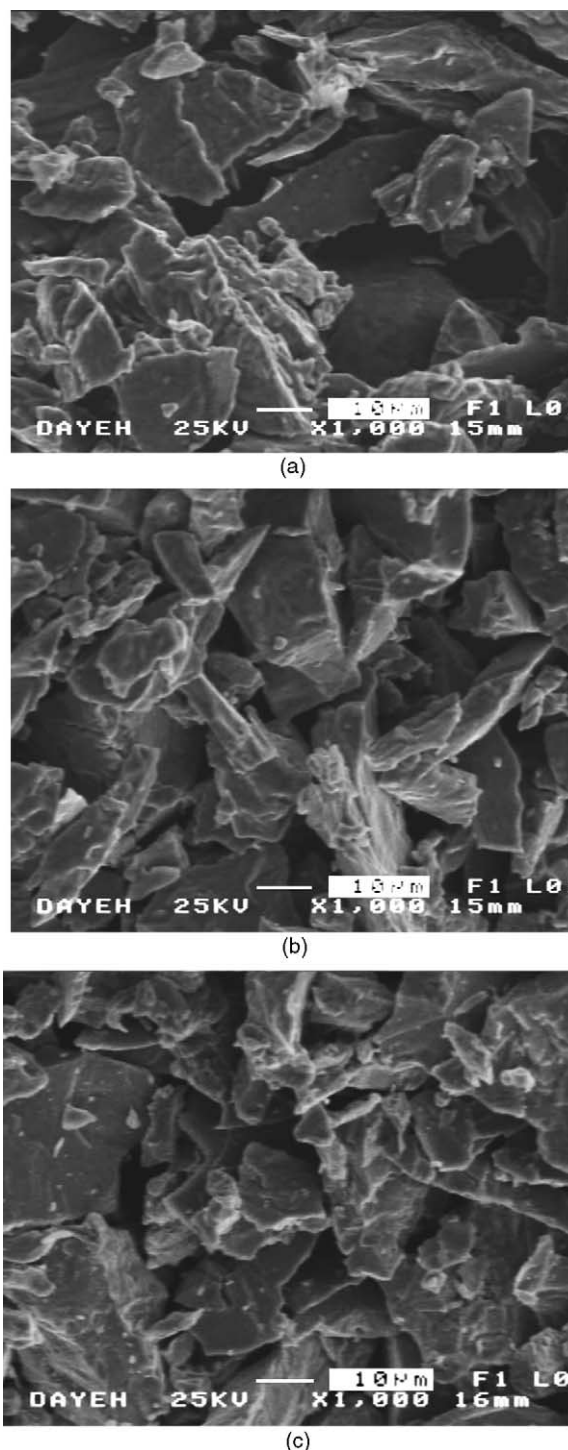


Fig. 13. SEM micrographs of an undiluted 50% TMD Nb sample nitrided in 1.3 MPa  $N_2$ : (a) near surface of sample; (b) halfway to center of sample; and (c) near center of sample.



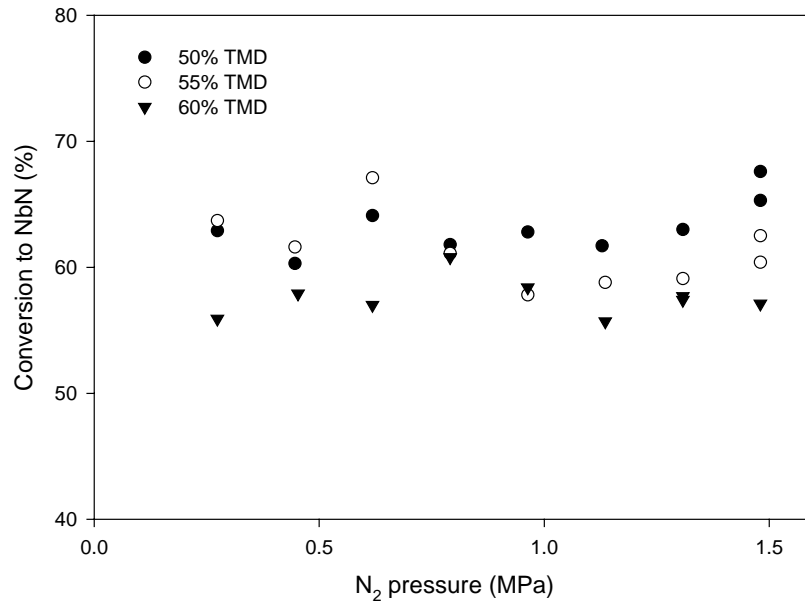


Fig. 14. Effects of nitrogen pressure and sample density on conversion percentage of undiluted Nb samples.

ple diluted with 25-wt.% NbN. This explains the observation that the self-sustained combustion cannot be achieved under the dilution with 30-wt.% NbN or higher.

A typical approach to the investigation of the mechanism of self-sustained reactions is through a determination of the dependence of the reaction front velocity on combustion temperature. Such a dependence is expressed in the following simplified form [10,13]:

$$\left(\frac{V_f}{T_c}\right)^2 = K \left(\frac{R}{E_a}\right) \exp\left(\frac{-E_a}{RT_c}\right)$$

where  $V_f$  is the velocity of the combustion wave,  $T_c$  is the combustion temperature,  $E_a$  is the activation energy of the process,  $R$  is the universal gas constant, and  $K$  is a constant which includes the heat capacity and density of the product and the heat of reaction. Fig. 12 shows a plot of  $\ln(V_f/T_c)^2$  versus  $1/T_c$  for samples nitrated by SHS under nitrogen pressures in the range from 0.27 to 1.5 MPa. From the slope of the best-fit line of all the data in Fig. 12, an activation energy,  $E_a$ , of 38.82 kJ/mol was calculated for the niobium/nitrogen SHS reaction.

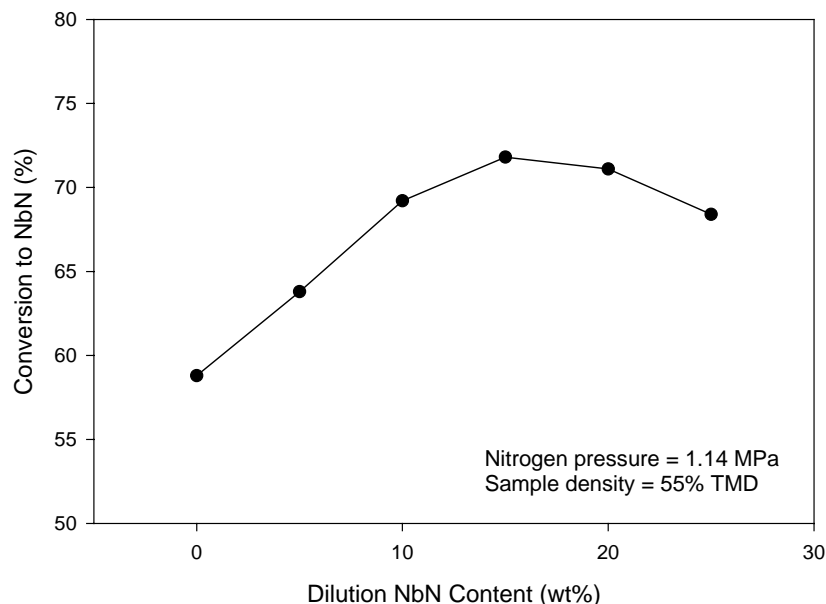


Fig. 15. Effect of diluent concentration on conversion percentage of Nb samples.

### 3.4. Analysis of product morphology and composition

The morphologies of a burned sample on locations near the sample surface, halfway between the surface and the center of the sample, and near the center are shown in Fig. 13a–c, respectively. SEM micrographs, first, reveal that the microstructures on three different locations are quite similar. In addition, compared with the reactant Nb powder, the particle morphology did not change after the SHS reaction. This not only suggests no melting of the niobium particle or product nitride, but also means without formation of any liquid phase during the SHS process. Therefore, the test sample

retained its porosity for the continuous filtration of nitrogen gas, leading to an afterburning stage.

The molar conversion percentage of niobium to nitride for the undiluted samples under different nitrogen pressures is shown in Fig. 14. The conversion percentages obtained in this study for the undiluted samples are approximately ranged between 56 and 70%. In general, the sample with a lower density yielded a slightly higher degree of conversion. No distinct dependence of the conversion percentage on the nitrogen pressure was found. This is mainly attributed to the afterburning reaction, in which the continuous nitridation takes place after the passage of the flame-front. The

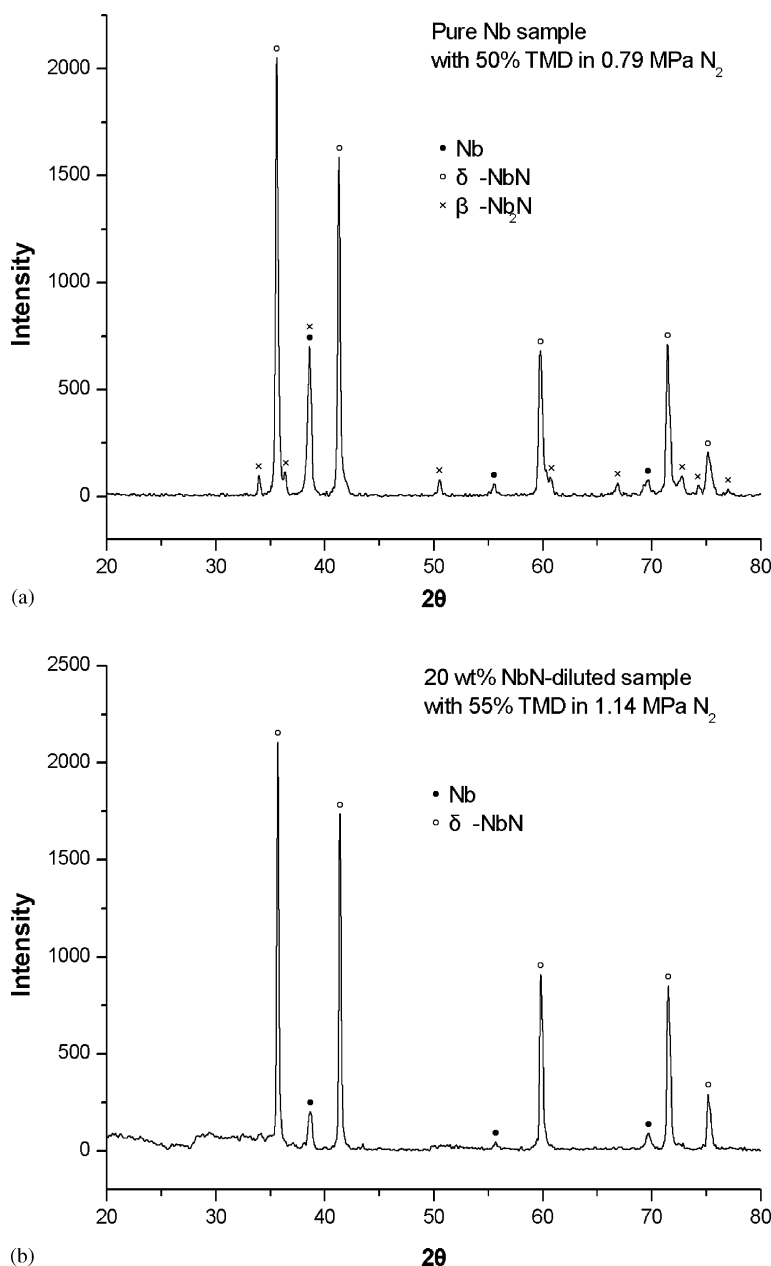


Fig. 16. XRD spectra of products obtained from (a) an undiluted sample nitrided in 0.79 MPa  $N_2$  and (b) a 20 wt.% NbN-diluted sample nitrided in 1.14 MPa  $N_2$ .

increase of conversion percentage by the addition of product NbN as a diluent is shown in Fig. 15. The conversion percentage was increased by increasing the diluent concentration up to 15 wt.%. Further increase in the diluent content led to a decrease in the conversion percentage, due to the decrease of combustion temperature. As shown in Fig. 15, an optimal increase of about 13% in the degree of conversion was obtained under 15-wt.% NbN dilution.

Typical X-ray diffraction (XRD) spectra of combustion products obtained from undiluted and NbN-diluted samples are shown in Fig. 16a and b, respectively. The XRD pattern in Fig. 16a represents a combination of three major species, including two nitride phases of  $\delta$ -NbN and  $\beta$ -Nb<sub>2</sub>N, as well as the unreacted Nb. The XRD analysis suggests that  $\delta$ -NbN is the dominant nitride product and the formation of the  $\beta$ -Nb<sub>2</sub>N is because of the insufficient nitrogen. As shown in Fig. 16b, the combustion product obtained from a 20-wt.% NbN-diluted sample was made up largely of  $\delta$ -NbN with a minor amount of Nb. No existence of  $\beta$ -Nb<sub>2</sub>N was found in the product of NbN-diluted samples.

#### 4. Conclusions

This study represents the first attempt to comprehensively describe the SHS process associated with niobium in nitrogen to form niobium nitride. The flame propagation mode of the Nb/N<sub>2</sub> SHS system is characterized by two consecutive combustion stages. The first stage showing the propagation of a planar front is contributed to the heat input from the igniter. The second stage featuring a spinning combustion wave traveling on the sample surface is believed to be the self-sustained combustion. In addition, an afterburning stage, where prolonged bulk combustion takes place, follows the passage of the flame-front. In agreement with the above observations, measured temperature profiles show a sharp increase signifying the arrival of the combustion wave, and a subsequent temperature rise representing the prolonged afterburning reaction. It was found that measured combustion temperatures in both flame propagation and afterburning periods were always lower than the melting points of either Nb or NbN.

Both the longitudinal and spinning front velocities increase with the nitrogen pressure, but decrease with the sample density. Moreover, the spinning wave propagates at one order of magnitude faster than does the longitudinal front. Based upon the measured flame velocities and combustion temperatures, an activated energy of 38.82 kJ/mol was obtained for the SHS reaction of niobium in gaseous nitrogen of 0.27–1.5 MPa.

Measured combustion temperatures, together with SEM micrographs, which show no change in the particle morphology after the combustion, verify without formation of any liquid phase. This implies that after the passage of the flame-front the sample still retains its porosity for nitrogen to penetrate, resulting in the afterburning reaction. For

the undiluted samples, the conversion percentages ranged between 56 and 70% were independent of the nitrogen pressure, since the nitridation continued to proceed in the afterburning stage. The addition of NbN as a diluent increases the degree of conversion. However, the reaction was quenched before reaching the self-sustained combustion for the samples diluted with 30-wt.% NbN or higher, due to a significant decrease in combustion temperature. An optimal increase of about 13% in the conversion percentage was obtained under 15-wt.% NbN dilution. The XRD analysis identified  $\delta$ -NbN as the dominant nitride phase synthesized in this study. For the undiluted samples, a small amount of  $\beta$ -Nb<sub>2</sub>N was found in the product.

#### Acknowledgements

This research was sponsored by the National Science Council of Taiwan, ROC, under grants of NSC 91-2212-E-212-020 and NSC 92-2212-E-212-003.

#### References

- [1] L.E. Toth, *Transition Metal Carbides and Nitrides*, Academic Press, New York, 1971.
- [2] A.G. Merzhanov, I.P. Borovinskaya, Self-propagating high-temperature synthesis of refractory inorganic compounds, *Doklady Akademii Nauk USSR* 204 (1972) 366–369.
- [3] Y. Saito, S. Kawata, H. Nakane, H. Adachi, Emission characteristics of niobium nitride field emitters, *Appl. Surf. Sci.* 146 (1999) 177–181.
- [4] Y. Gotoh, M. Nagao, T. Ura, H. Tsuji, J. Ishikawa, Ion beam assisted deposition of niobium nitride thin films for vacuum microelectronics devices, *Nucl. Instrum. Methods Phys. Res. B* 148 (1999) 925–929.
- [5] J.J. Moore, H.J. Feng, Combustion synthesis of advanced materials: Part I. Reaction parameters, *Progr. Mater. Sci.* 39 (1995) 243–273.
- [6] A.G. Merzhanov, History and recent development in SHS, *Ceram. Int.* 21 (5) (1995) 371–379.
- [7] J.J. Moore, H.J. Feng, Combustion synthesis of advanced materials: Part II. Classification, applications, and modelling, *Progr. Mater. Sci.* 39 (1995) 275–316.
- [8] C.C. Agrafiotis, J.A. Puszynski, V. Hlavacek, Experimental study on the synthesis of titanium and tantalum nitrides in the self-propagating regime, *Combust. Sci. Technol.* 76 (1991) 187–218.
- [9] M. Eslambo-Grami, Z.A. Munir, Effect of nitrogen pressure and diluent content on the combustion synthesis of titanium nitride, *J. Am. Ceram. Soc.* 73 (1990) 2222–2227.
- [10] M. Eslambo-Grami, Z.A. Munir, Effect of porosity on the combustion synthesis of titanium nitride, *J. Am. Ceram. Soc.* 73 (1990) 1235–1239.
- [11] H. Kudo, O. Odawara, Characteristics of self-propagating reaction in TiN combustion synthesis, *J. Mater. Sci.* 24 (1989) 4030–4033.
- [12] C.L. Yeh, H.C. Chuang, Combustion characteristics of SHS process of titanium nitride with TiN dilution, *Ceram. Int.*, 30 (2004) 705–714.
- [13] S. Zhang, Z.A. Munir, The combustion synthesis of refractory nitrides, Part II: The synthesis of niobium nitride, *J. Mater. Sci.* 26 (1991) 3380–3385.
- [14] C.C. Agrafiotis, J.A. Puszynski, V. Hlavacek, Effect of metal particle morphology on the combustion of refractory metals in nitrogen, *J. Am. Ceram. Soc.* 74 (1991) 2912–2917.
- [15] T.P. Ivleva, A.G. Merzhanov, Three-dimensional spinning waves in the case of gas-free combustion, *Doklady Phys.* 45 (2000) 136–141.